

Pulsed laser crystallization of very thin silicon films

T. Sameshima^{a,*}, H. Watakabe^a, N. Andoh^a, S. Higashi^b

^a*Tokyo University of Agriculture and Technology, Koganei, Tokyo 184-8588, Japan*

^b*Hiroshima University, Higashi-Hiroshima 739-8530, Japan*

Available online 29 March 2005

Abstract

We report 308-nm-pulsed-XeCl-excimer laser annealing of 2.2-nm-thick silicon films formed on quartz substrates. Crystallization occurred at laser energy of 150–170 mJ/cm². Raman scattering spectra revealed mixed states of small crystalline grains and disordered amorphous regions. Broad optical extinction coefficient was obtained for wavelength from 250 to 400 nm, although it was similar to that of crystalline silicon for wavelength longer than 400 nm. Blue-green photoluminescence was observed for the films annealed at 260 °C for 3 h in 1.3×10⁶ Pa H₂O vapor after crystallization.

© 2005 Elsevier B.V. All rights reserved.

Keywords: Crystallization; Disordered states; Nano-crystalline; Photoluminescence

1. Introduction

Pulsed laser crystallization of silicon has been precisely studied [1–7]. Laser-induced melt followed by solidification has been analyzed. Moreover, pulsed laser crystallization has been widely applied to formation of polycrystalline silicon films and has been introduced to fabrication process of polycrystalline silicon thin film transistors (poly-Si TFTs) [8–15]. Formation of crystalline silicon films with thickness from 20 to 100 nm has been established by pulsed laser crystallization. High crystalline volume ratio and crystalline grains with excellent properties have been obtained. Pulsed laser crystallization of nanometer-order thin films is interesting in the formation of nanometer-size crystalline grains with having low-dimensional-quantum effect properties. However, few researches on laser crystallization of very thin silicon films have been carried out [16].

In this paper, we report pulsed XeCl excimer laser crystallization of 2.2-nm-thick silicon films formed on glass substrates. Physics of laser crystallization of thin silicon films is discussed. Structural properties are also discussed. Ultraviolet light-induced photo luminescence is reported.

2. Experiments

2.2-nm-thick undoped amorphous silicon films were formed on quartz glass substrates at 300 °C by plasma enhanced chemical vapor deposition (PECVD) methods. The thickness was determined by the deposition rate and the optical reflectivity of the sample surface at 800 nm. The samples were irradiated with 308-nm-pulsed-XeCl-excimer laser at room temperature in vacuum with different pulse energies. Raman scattering was measured for structural analysis using a probe laser light at 514.5 nm with 4 mW and 5- μ m diameter. Optical transmissivity and reflectivity spectra were also measured in visible and ultraviolet ranges. 1.3×10⁶ Pa H₂O vapor heat treatment [17] was carried out to reduce defects in disordered states for samples coated with 76 nm SiO_x films thermally evaporated on the film surface. Photo luminescence was also observed with high-sensitive CCD camera at room temperature by 30 mJ/cm² XeCl excimer laser excitation with a beam area of 1 mm×1 mm.

3. Pulsed laser heating of silicon films

Silicon films can be rapidly melted by pulsed laser irradiation, which then solidified to crystalline phase after

* Corresponding author.

E-mail address: tsamesim@cc.tuat.ac.jp (T. Sameshima).

irradiation. Melting initiates when the silicon surface is heated above the melting point. Molten region extends in deep region when the latent heat energy for melting is given by laser energy. Because the latent heat of silicon is 4171 J/cm^3 [18], high laser energy was required to melt silicon films deep. Heat flow simulation was conducted to calculate the required energy for melting silicon films. Fig. 1 shows threshold heating energies per unit area for increasing temperature at the silicon surface to the melting point and for giving the latent heat energy in the whole thickness, which means complete melting, as a function of the film thickness. The threshold energies were calculated by numerical heat flow calculation program using data of intensity change of our XeCl excimer laser pulse. No energy losses such as surface reflection were considered. The threshold energy of heating the surface to the melting point is almost independent of the film thickness because the heat diffusion length is $\sim 300 \text{ nm}$ at the termination of laser pulse. The length was much larger than the film thickness. On the other hand, the threshold energy for complete melting increased as the film thickness increased because the latent heat energy per unit area for changing the solid state to the liquid state is proportional to film thickness. For energy between the two thresholds, the interface control growth occurs; the melt region extends and the melt–solid interface proceeds into deep regions during laser heating. After the termination of laser pulse, the interface moves up to the surface according to heat diffusion into the substrate. Polycrystalline silicon grains have been formed from the nucleation sites localized the bottom surface. The grain size is roughly limited by film thickness. For thickness from 20 nm to 50 nm, silicon films are crystallized well and a high crystalline volume ratio 0.9 is obtained. On the other hand, undercooling liquid state occurs after laser irradiation for laser energy above the complete melting threshold. Liquid silicon with temperature much lower than the melting point is rapidly solidified to amorphous state or very small crystalline grains. Laser-induced amorphization has been observed for film thickness from 6 to 20 nm [16]. However,

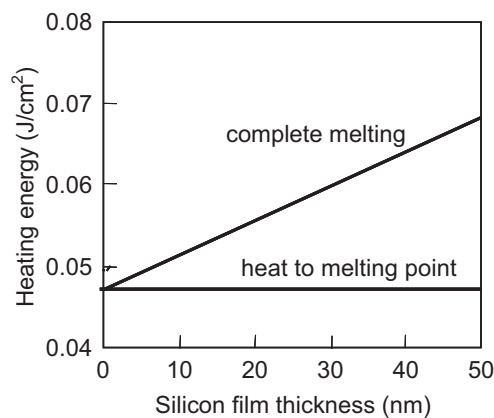


Fig. 1. Threshold heating energies per unit area for increasing temperature at the silicon surface to the melting point and complete melting of the films as a function of the film thickness.

interface control growth and melt followed by amorphization have been not reported yet for silicon films thinner than 6 nm. The heat flow calculation suggests that window of the laser energy is very narrow for crystallization of 2-nm-thick silicon films.

4. Experimental results and discussion

Fig. 2 shows Raman Stokes spectra silicon films initial amorphous and laser annealed with different energies. Although the initial film had only a broad peak from 400 to 500 cm^{-1} , small and sharp peak appeared around 516 cm^{-1} of TO phonon of crystalline silicon for laser irradiation at 150 mJ/cm^2 . The crystalline TO phonon peak intensity increased and amorphous broad band intensity decreased for laser irradiation at 160 and 170 mJ/cm^2 . On the other hand, crystalline TO phonon peak intensity markedly decreased for laser irradiation at 180 mJ/cm^2 and amorphous broad band increased. These results show that silicon films were crystallized by laser irradiation from 150 to 170 mJ/cm^2 , and that they are amorphized at laser irradiation higher than 180 mJ/cm^2 . It is the same behavior of laser-induced melt followed by solidification of thick silicon films described above. The energy window for crystallization is about 30 mJ/cm^2 . It is much smaller than 300 mJ/cm^2 , the energy window for 50-nm-thick films, which we determined previously [19].

Although silicon films 20 to 50 nm thick can be almost completely crystallized, 2.2-nm-crystallized silicon films had strong broad band at low wave number in Raman spectra as shown in Fig. 2. This means that thin laser crystallized silicon films had significant disordered states. Analysis of the spectrum by fitting with Gaussian curve for 170 mJ/cm^2 crystallized films resulted in that spectrum had three peaks. The peak wave number, width and peak intensity are listed below in Table 1. The band width of crystalline TO phonon was broad of 6 cm^{-1} and there was a peak with a high intensity around 500 cm^{-1} . These results suggest that crystalline grains with very small size approximately nanometers were formed by laser irradiation [20,21]. Silicon melting has a possibility of movement of Si atoms because of surface tension of liquid silicon on quartz, although the melting duration was very short. Globular shape crystalline grains with their diameters larger than the films thickness would be formed and they would result in sharp Raman peak at 516 cm^{-1} .

We estimated the optical extinction coefficient, which depends on the densities of state of valence and conduction bands, by analysis of optical reflectivity and transmissivity spectra using numerical calculation program with fresnel coefficient of layered structure of 2.2-nm-thick films formed on quartz. Fig. 3 shows the optical extinction coefficient spectra for films laser annealed at 170 and 190 mJ/cm^2 as well as amorphous and crystalline silicon for comparison. For laser energy at

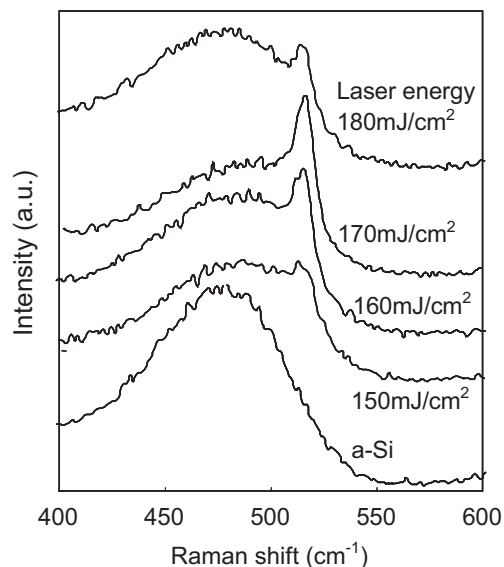


Fig. 2. Raman Stokes spectra silicon films initial amorphous and laser annealed with different energies.

170 mJ/cm², the optical extinction coefficient was low value near that of crystalline silicon for long wavelength region from 400 to 750 nm. Dielectric response was similar to that of bulk crystalline silicon at the long wavelength region. On the other hand the optical extinction coefficient was far different from that of crystalline silicon at wavelength 250 to 400 nm. E₁ and E₂ singular peaks associated four fold tetrahedral bonding states decreased. These indicates three dimensional crystalline band structure was changed by the thickness limitation of 2.2 nm. Substantial optical extinction was observed for wavelength from 400 to 750 nm for films irradiated at 190 mJ/cm² and very broad extinction spectra appeared at wavelength 250 to 400 nm. These results mean that there were disordered amorphous states like amorphous silicon.

Photoluminescence was also observed. Fig. 4 shows photographs of photo emission at irradiation of excimer laser pulse at 30 mJ/cm² at room temperature for 170 mJ/cm² laser annealed films. Although no emission was observed for as crystallized films, blue-green light emission was observed for films treated at 260 °C with 1.3×10⁶ Pa H₂O vapor. Through effective reduction of non-irradiative energy relaxation defect sites by H₂O heat treatment, optical emission occurred probably via direct energy transition in low-dimensional band structure in small crystalline grains.

Table 1
Peak wave number, width and peak intensity analyzed by Gaussian fitting for 170 mJ/cm² crystallized films. The instrument resolution is 4 cm⁻¹

	Peak 1	Peak 2	Peak 3
Peak wave number (cm ⁻¹)	516	500	460
Width (cm ⁻¹)	6	30	55
Intensity (a.u.)	1.0	1.2	1.5

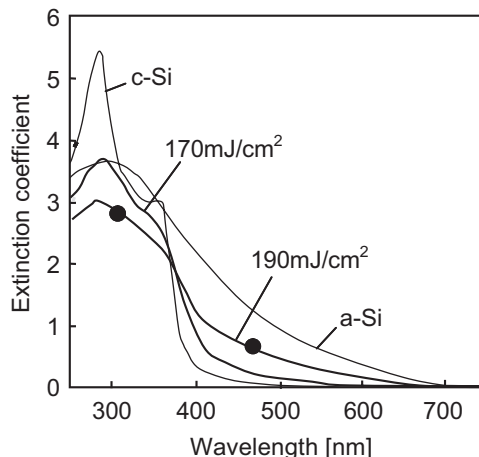
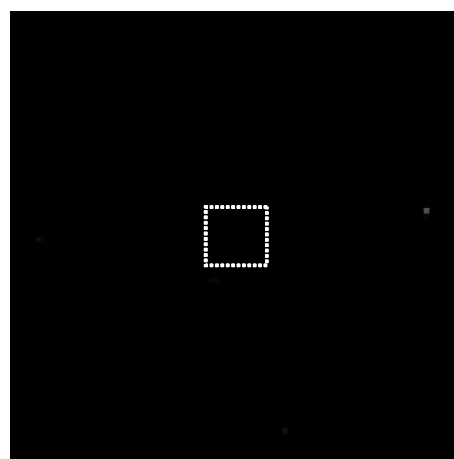
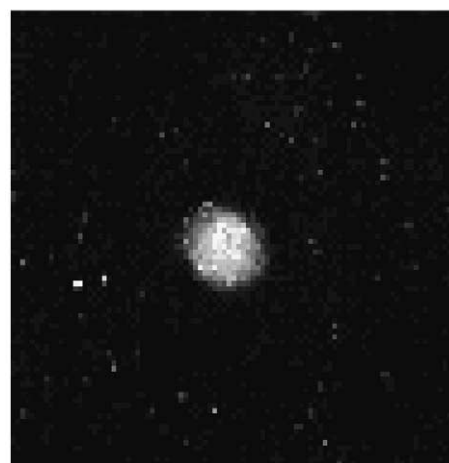


Fig. 3. The optical extinction coefficient spectra for films laser annealed at 170 and 190 mJ/cm² and amorphous and crystalline silicon for comparison.



(a)



(b)

Fig. 4. Photographs of photo emission at irradiation of excimer laser at 30 mJ/cm² for sample as laser irradiated at 170 mJ/cm² (a). The white square shows the area of laser irradiation with 1 mm×1 mm. Photographs (b) shows photo emission after 1.3×10⁶ Pa H₂O vapor heat treatment 260 °C for 3 h.

5. Summary

We investigated 308-nm-pulsed-XeCl-excimer laser annealing of 2.2-nm-thick silicon films formed on quartz substrates. Laser-induced crystallization occurred at laser energy of 150–170 mJ/cm². Laser-induced amorphization was observed for laser irradiation above 180 mJ/cm². Analysis of Raman scattering spectra revealed that there was three *TO* phonon bands at 516 cm⁻¹, 500 cm⁻¹ and 500 cm⁻¹ for films annealed at 170 mJ/cm². It indicates that the films had small crystalline grains and disordered amorphous regions. Broad optical extinction coefficient was obtained for wavelength from 250 to 400 nm, although it was similar to that of crystalline silicon for wavelength longer than 400 nm. Blue-green photoluminescence was observed for the films annealed at 260 °C for 3 h in 1.3×10⁶ Pa H₂O vapor after crystallization, although no photoemission was observed for as-crystallized silicon films. Defect states were effectively reduced by H₂O heat treatment. Optical emission occurred probably via direct energy transition in low-dimensional band structure in small crystalline grains.

References

- [1] R.F. Wood, C.E. Giles, Phys. Rev., B 23 (1981) 2923.
- [2] R.F. Wood, C.E. Giles, Phys. Rev., B 23 (1981) 5555.
- [3] D.H. Lowndes, G.H. Kirkpatrick Jr., S.J. Pennycook, S.P. Withrow, D.N. Mashburn, Appl. Phys. Lett. 48 (1986) 1389.
- [4] P.L. Liu, R. Yen, N. Bloembergen, R.T. Hodson, Appl. Phys. Lett. 34 (1979) 864.
- [5] R. Tsu, R.T. Hodgson, T.Y. Tan, J.E. Baglin, Phys. Rev. Lett. 42 (1979) 1356.
- [6] T.F. Deutsch, J.C.C. Fan, C.W. Turner, R.L. Chapman, D.J. Ehrlich, R.M. Osgood Jr., Appl. Phys. Lett. 38 (1981) 144.
- [7] S. Higashi, T. Sameshima, Jpn. J. Appl. Phys. 40 (2001) 480.
- [8] T. Sameshima, S. Usui, M. Sekiya, IEEE Electron Device Lett. EDL-7 (1986) 276.
- [9] K. Sera, F. Okumura, H. Uchida, S. Itoh, S. Kaneko, K. Hotta, IEEE Trans. Electron Devices 36 (1989) 2868.
- [10] H. Kuriyama, T. Kuwahara, S. Ishida, T. Nohda, K. Sano, H. Iwata, S. Noguchi, S. Kiyama, S. Tsuda, S. Nakano, M. Osumi, Y. Kuwano, Jpn. J. Appl. Phys. 31 (1992) 4550.
- [11] E.L. Mathé, J.G. Maillou, A. Naudon, E. Fogarassy, M. Elliq, S. De Unamuro, Appl. Surf. Sci. 43 (1989) 142.
- [12] A. Kohno, T. Sameshima, N. Sano, M. Sekiya, M. Hara, IEEE Trans. Electron Devices ED-42 (1995) 251.
- [13] S. Uchikoga, N. Ibaraki, Thin Solid Films 383 (2001) 19.
- [14] S. Higashi, K. Ozaki, K. Sakamoto, Y. Kano, T. Sameshima, Jpn. J. Appl. Phys. 38 (1999) L857.
- [15] S. Higashi, D. Abe, S. Inoue, T. Shimoda, Jpn. J. Appl. Phys. 40 (2001) 4171.
- [16] T. Sameshima, S. Usui, Appl. Phys. Lett. 59 (1991) 2724.
- [17] T. Sameshima, M. Satoh, Jpn. J. Appl. Phys. 36 (1997) L687.
- [18] L.V. Gurvich, I.V. Veyts, Thermodynamic properties of individual substances, Hemisphere Publishing Corporation, New York, (1991) p. 237, 308.
- [19] T. Sameshima, K. Saitoh, N. Aoyama, S. Higashi, M. Kondo, A. Matsuda, Jpn. J. Appl. Phys. 38 (1999) 1892.
- [20] H. Richter, Z.P. Wang, L. Ley, Solid State Commun. 39 (1981) 625.
- [21] G. Viera, S. Huet, L. Boufendi, J. Appl. Phys. 90 (2001) 4175.